

# Microstructure and Electrical Properties of Pb[(Mg,Mn)Nb]O<sub>3</sub>-Pb(Zr,Ti)O<sub>3</sub> Piezoelectric Ceramics

Jin-Ho Kim<sup>a</sup> and Jong-Hwa Kim

*Department of Inorganic Materials Engineering, Kyungpook National University,  
1370 Sankyuk-dong, Buk-gu, Daegu 702-701, Korea*

Seung-Woo Baik

*Department of Material-processing Eng. & Applied Chemistry for Environment,  
Faculty of Engineering and Resource Science, Akita University,  
1-1 Tegata-Gakuen cho, Akita 010-8502, Japan*

<sup>a</sup>E-mail : [jihkim@mail.knu.ac.kr](mailto:jihkim@mail.knu.ac.kr)

(Received August 6 2005, Accepted September 6 2005)

Phase evolution, microstructure and the electrical properties such as  $k_p$  and  $Q_m$  of Pb(Mg<sub>1/3</sub>Nb<sub>2/3</sub>)O<sub>3</sub>[PMN]-Pb(Mn<sub>1/3</sub>Nb<sub>2/3</sub>)O<sub>3</sub>[PM'N]-PbZrO<sub>3</sub>[PZ]-PbTiO<sub>3</sub>[PT] quaternary system were investigated within the compositional ranges  $0 \leq y \leq 0.125$ ,  $y+z=0.125$ , and  $0.39 \leq x \leq 0.54$  of the formula Pb<sub>0.97</sub>Sr<sub>0.03</sub>[(Mg<sub>1/3</sub>Nb<sub>2/3</sub>)<sub>y</sub>(Mn<sub>1/3</sub>Nb<sub>2/3</sub>)<sub>z</sub>(Zr<sub>x</sub>Ti<sub>1-x</sub>)<sub>1-(y+z)</sub>]O<sub>3</sub>. In the case of increasing Mn/(Mg+Mn) ratio for a fixed Zr/Ti ratio of 47.5/52.5, phase relation remained unchanged but the grain size drastically decreased, and the electrical properties changed as following: both  $k_p$  and  $Q_m$  reached the peak values at Mn/(Mg+Mn)≅0.317 and gradually decreased;  $\epsilon_{33}^T$  showed a monotonic decrease; P-E hysteresis loop gradually changed to asymmetrical one, and  $E_i$  increased in correspondence. With increasing Zr/Ti ratio for a fixed Mn/(Mg+Mn) ratio of 0.317, on the contrary, the cell parameter  $(a^2c)^{1/3}$  gradually increased, and tetragonal-rhombohedral morphotropic phase boundary appeared in the range of  $51/49 \leq Zr/Ti \leq 54/46$ . In the meantime, the grain size substantially increased, and the electrical properties changed as following:  $k_p$  and  $\epsilon_{33}^T$  reached peak values at Zr/Ti=51/49 and 48/52, respectively, and then gradually decreased; change of  $Q_m$  was adverse to  $k_p$ ; both  $E_C$  and  $E_i$  considerably decreased while  $P_S$  moderately increased. For the system 0.125(PMN+PM'N)-0.875PZT studied, the composition Mn/(Mg+Mn)=0.317 and Zr/Ti=51/49 revealed some promising electrical properties for piezoelectric transformer application such as  $k_p=0.58$ ,  $Q_m \cong 1000$ , and  $\epsilon_{33}^T=970$ , as well as dense and fine-grained microstructure.

**Keywords :** Piezoelectric ceramics, Phase evolution, Microstructure, Piezoelectric constants

## 1. INTRODUCTION

Since Jaffe et al. reported the discovery of the piezoelectric ceramic Pb(Zr,Ti)O<sub>3</sub> (abbreviated as PZT) in 1954[1], much efforts have been devoted to basic research on PZT and PZT-based ferroelectric materials. Smolenskii et al. first reported the synthesis of complex perovskite-type ferroelectrics such as Pb(Fe<sub>1/2</sub>Ta<sub>1/2</sub>)O<sub>3</sub> and Pb(Mg<sub>1/3</sub>Nb<sub>2/3</sub>)O<sub>3</sub>, which had extensive influence on the development of piezoelectric ceramics[2]. In 1970's many complex perovskite-type piezoelectric ceramics based on the formula Pb<sup>2+</sup>(M<sup>+2</sup><sub>1/3</sub>M<sup>+5</sup><sub>2/3</sub>)O<sub>3</sub>, Pb<sup>2+</sup>(M<sup>+3</sup><sub>1/2</sub>M<sup>+5</sup><sub>1/2</sub>)O<sub>3</sub> and Pb<sup>2+</sup>(M<sup>+2</sup><sub>1/2</sub>M<sup>+6</sup><sub>1/2</sub>)O<sub>3</sub> were proposed (M, M' are B-site cations in perovskite

structure such as Co<sup>2+</sup>, Mg<sup>2+</sup>, Ni<sup>2+</sup>, Fe<sup>3+</sup>, Mn<sup>3+</sup>, Sb<sup>3+</sup>, Sb<sup>5+</sup>, Nb<sup>5+</sup>, W<sup>6+</sup>), and hundreds of ternary and multi-component piezoelectric ceramics are available nowadays[3]. It is believed that many more new piezoelectric ceramic materials will be found in the future.

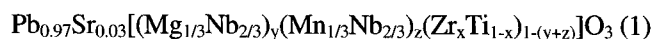
The applications of piezoelectric ceramics have included electroacoustic transformers and signal-processing devices, and are presently reaching to the field of optical-path control systems and precision motors incorporating piezoelectric actuators[3]. The use of piezoelectric materials to modern industry meets the technological needs for the miniaturization and high efficiency of a variety of electronic equipments, as is

clearly shown in the example of piezoelectric ceramic transformers; their simple structure and miniaturized size compared with the traditional coil transformers make these transducers preferable for high voltage DC power supplies of TV receivers and monitors and especially for backlight inverters of LCD panels of notebook computers in accordance with the advancement of information technology[4]. The prerequisites of piezoelectric ceramics for DC transducer application are: high electromechanical coupling factor,  $k_p$ , of  $\geq 0.6$ ; high mechanical quality factor,  $Q_m$ , of  $\geq 1000$ ; low dielectric loss; low degradation in piezoelectricity; dense and fine-grained microstructure for high mechanical strength. Several Pb-based ternary and quaternary systems have been proposed as promising piezoelectric materials for ceramic transducers:  $\text{Pb}(\text{Mg}_{1/3}\text{Nb}_{2/3})\text{O}_3\text{-PZT}$ , named PCM[5];  $\text{Pb}(\text{Mn}_{1/3}\text{Sb}_{2/3})\text{O}_3\text{-PZT}$ , named PMS[6];  $\text{Pb}(\text{Sb}_{1/2}\text{Nb}_{1/2})\text{O}_3\text{-PZT}$ [7]. Previous investigations of these systems, however, focused mainly on their device applications for ceramic transformers, so that comprehensive understandings of the influences of phase evolution and microstructure on piezoelectricity of these systems are presently not attained. Particularly in  $\text{Pb}(\text{Mg}_{1/3}\text{Nb}_{2/3})\text{O}_3\text{-Pb}(\text{Mn}_{1/3}\text{Nb}_{2/3})\text{-PZT}$  system, no detailed study about the correlation among the composition, microstructure and piezoelectricity has been reported so far.

In the present work, the influence of composition on phase evolution, ceramic microstructure and piezoelectric properties of  $\text{Pb}(\text{Mg}_{1/3}\text{Nb}_{2/3})\text{O}_3\text{-Pb}(\text{Mn}_{1/3}\text{Nb}_{2/3})\text{-PZT}$  quaternary system have been thoroughly investigated. The morphotropic phase boundary (MPB) of the system has been defined as a function of Zr/Ti ratio, and the effect of Mn/Mg ratio on microstructure has also been studied. On the whole, optimal composition and processing parameters of the system have been suggested for piezoelectric transformer application.

## 2. EXPERIMENT

Reagent grade ( $\geq 99.9\%$ )  $\text{PbO}$ ,  $\text{ZrO}_2$ ,  $\text{TiO}_2$ ,  $\text{Nb}_2\text{O}_5$ ,  $\text{MgO}$  and commercial grade ( $\geq 99.5\%$ )  $\text{Mn}_3\text{O}_4$ ,  $\text{SrCO}_3$  powders were used as raw materials. Nominal compositions of the quaternary system (hereafter abbreviated as PMM'NZT, where  $M=\text{Mg}$  and  $M'=\text{Mn}$ ) can be expressed as:



where  $0 \leq y \leq 0.125$ ,  $y+z=0.125$ , and  $0.39 \leq x \leq 0.54$ . The values of  $x$  and  $y$  were changed at the regular intervals of  $\Delta x=0.03$  and  $\Delta y=0.0066$ . In each batch formulation, 3 at% of Sr were substituted for Pb for improved piezoelectric properties[8], and 3 wt% excess PbO were

added to compensate for the Pb loss in firing. Figure 1 represents the schematic diagram of sample preparation. The B-site precursor method[9] was used in the preparation of PMM'NZT: firstly the mixtures of  $\text{ZrO}_2$ ,  $\text{TiO}_2$ ,  $\text{MgO}$ ,  $\text{Mn}_3\text{O}_4$ , and  $\text{Nb}_2\text{O}_5$  in given ratios were calcined at  $1050\text{ }^\circ\text{C}$  for 2 h, and pulverized with prescribed amount of  $\text{PbO}$  and  $\text{SrCO}_3$ ; dried admixtures were calcined again at  $850\text{ }^\circ\text{C}$  for 2 h, and then pulverized. Powder pulverization was performed by wet-ballmilling with ethanol for 20 h using a plastic jar and 5 mm $\Phi$  YTZ balls. After drying and adding PVA solution, the milled calcines were granulated to pass a 100-mesh sieve. Granules were uniaxially pressed under 10 MPa into disks of 15 mm in diameter and 3 mm thick, and then CIPed under 150 MPa. After binder burn-out at  $500\text{ }^\circ\text{C}$ , specimens were set in an  $\text{Al}_2\text{O}_3$  sagger and sintered between  $1100\text{ }^\circ\text{C}$  and  $1200\text{ }^\circ\text{C}$  for 2 h. To provide a PbO atmosphere in three disks separated by a sprinkle of coarse  $\text{ZrO}_2$  sintering, each stack of powder were put in a crucible and capped with a lid both made of PZT(52/48).

Fired density was obtained by Archimedes' method. Microstructures of polished and chemically etched specimens were examined using a SEM (JSM5400, JEOL). Phase evolution was studied with an x-ray diffractometer (M03-XHF, MacScience) using  $\text{CuK}\alpha$  radiation, and the lattice parameters were calculated using (002) and (200) peak positions on the diffraction profiles. Fired disks were thinned to 1 mm thickness and electroded on both sides by printing and firing of Ag-paste, and then poled with a dc electric field (30 kV/cm)

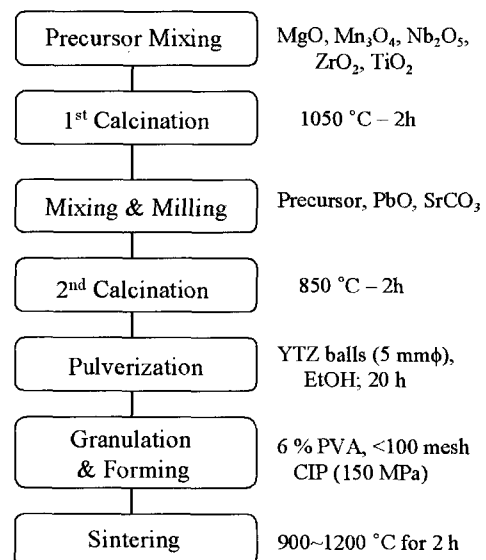


Fig. 1. Schematic diagram of sample preparation.

for 30 min in a silicone oil bath at 130 °C. Twenty-four hours after poling, the dielectric and piezoelectric properties were measured using an impedance/gain-phase analyzer (HP 4194A) according to the IRE standards[10]. And the P-E hysteresis loop was obtained with a Sawyer-Tower circuit (RT-66A) in a 60 Hz ac field of 50 kV/cm peak.

### 3. RESULTS AND DISCUSSION

According to a preliminary XRD study, only single perovskite phase existed in all the double-calcined PMM'NZT powders, indicating the completion of phase evolution. The diffraction peak positions, however, depended on the batch formulations. Figure 2(a) shows the change of tetragonal (002)-(200) diffraction profile of PMM'NZT (Zr/Ti = 47.5/52.5) with Mn/(Mg+Mn) ratio, sintered at 1100 °C. All the specimens exhibit similarly separated tetragonal (002) and (200) peaks in correspondence with the phase equilibrium of PbTiO<sub>3</sub>-

PbZrO<sub>3</sub>[11]. It seems, however, that the diffraction angles of (002) and (200) approach slightly to each other at high ratios of Mn/(Mg+Mn) near 1.0. To quantify this change, lattice parameters  $a$ ,  $c$ , and  $(a^2c)^{1/3}$  of the tetragonal structure are calculated and plotted as a function of Mn/(Mg+Mn) ratio in Fig. 2(b). It is evident that the lattice parameter  $c$  decreases slightly while  $a$  remains virtually unchanged with increasing Mn content, which results in the slight decrease of the average cell-size parameter  $(a^2c)^{1/3}$ . The volumetric contraction of tetragonal cell at high Mn/(Mg+Mn) ratio can be well explained by the difference in ionic radii (CN=6) of Mn<sup>2+</sup> and Mg<sup>2+</sup> (0.067 nm and 0.072 nm, respectively)[12].

Similar relation between Zr/Ti ratio and the diffraction profile of PMM'NZT (Mn/(Mg+Mn)=0.317), sintered at 1100 °C, is shown in Fig. 3(a), and the tetragonal cell parameters  $a$ ,  $c$  and pseudocubic parameter  $a$  of rhombohedral phase are plotted as a function of Zr/Ti ratio in Fig. 3(b). In the compositional range of 39/61 ≤ Zr/Ti ≤ 48/52, only tetragonal (002)-(200) peaks

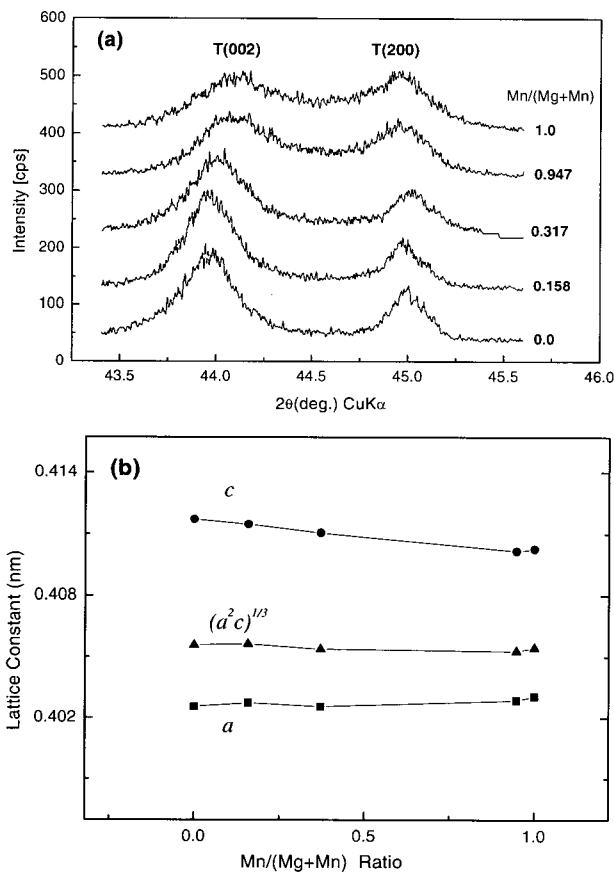


Fig. 2. Changes in (a) XRD peak profile of tetragonal (200) and (002), and (b) the corresponding tetragonal lattice parameters  $a$ ,  $c$  and  $(a^2c)^{1/3}$  of 0.125PMM'N-0.875PZT (Zr/Ti=47.5/52.5) with Mn/(Mg+Mn) ratio, sintered at 1150 °C for 2 h.

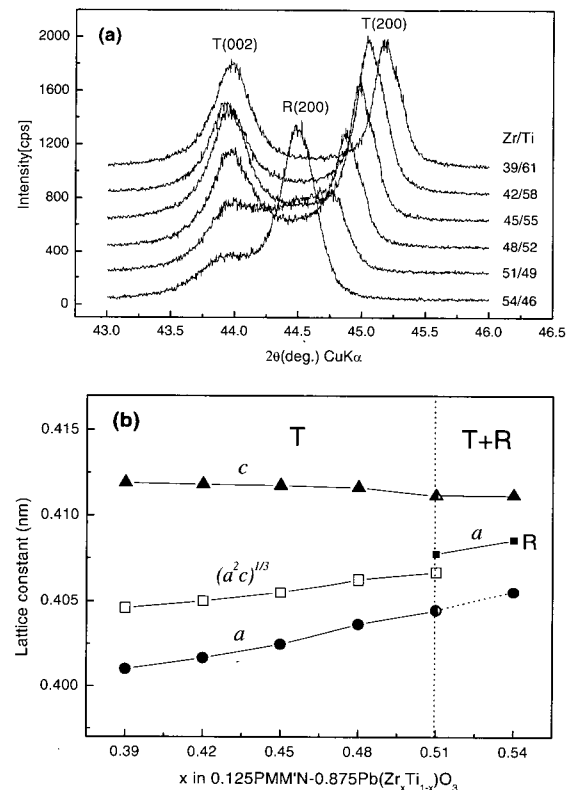


Fig. 3. Changes in (a) XRD peak profile of tetragonal (200)-(002) and rhombohedral (200), and (b) the corresponding lattice parameters  $a$ ,  $c$  and  $(a^2c)^{1/3}$  of tetragonal phase and  $a$  of rhombohedral (pseudocubic) phase of 0.125PMM'N-0.875PZT (Mn/(Mg+Mn)=0.317) with Zr/Ti ratio, sintered at 1150 °C for 2 h.

are present in the profile. In the composition of Zr/Ti=51/49, on the contrary, rhombohedral (200) peak appears in between tetragonal (002) and (200) peaks, and becomes predominant when Zr/Ti=54/46. With increasing Zr/Ti ratio, the lattice parameter *a* increases steadily while *c* barely increases. The composition of PZT where tetragonal and rhombohedral phases coexist is called MPB (morphotropic phase boundary), and is known to exist at  $Zr/Ti \cong 52/48$ . Although the nature of the MPB is still controversial, it is now well recognized that the MPB does not confined to a specific composition but expands to a compositional range over several mole percents or even more[13,14]. In the present PMM'NZT system, XRD study indicates that the compositional range  $51/49 \leq Zr/Ti \leq 54/46$  is included in the MPB, which is not significantly influenced by Mn/(Mg+Mn) ratio.

Figure 4 illustrates SEM photographs showing the effects of Mn/(Mg+Mn) and Zr/Ti ratios on the grain growth of PMM'NZT, sintered at 1150 °C for 2 h. Similar to pure PZT, the specimen 0.125PMN-0.875PZT (Zr/Ti=47.5/52.5, (a)) consisted of large ( $\geq 10 \mu\text{m}$ ) grains entrapping micropores and grain boundary pores. With

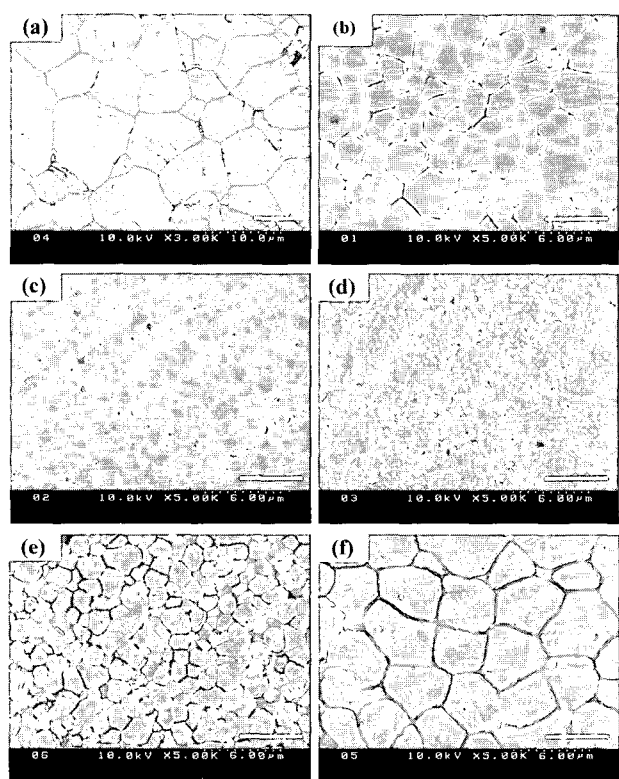


Fig. 4. SEM photographs of 0.125PMM'N-0.875PZT sintered at 1150 °C for 2 h. Mn/(Mg+Mn) ratios are: (a) 0.0 (PMN); (b), (e) and (f) 0.317; (c) 0.739; (d) 1.0 (PM'N). Zr/Ti ratios are: (a)-(d) 47.5/52.5; (e) 39/61; (f) 54/46 (bar = 5  $\mu\text{m}$ ).

increasing its Mn content, the grain size drastically decreased, and as a result the specimen 0.125PM'N-0.875PZT (d) had extraordinarily fine-grained ( $\sim 1 \mu\text{m}$ ) microstructure. In Mn/(Mg+Mn)=0.317 composition, on the contrary, increasing its Zr/Ti ratio in the order of 39/61 (e), 47.5/52.5 (b) and 54/46 (f), substantial increase in the grain size was observed. The drastic decrease of grain size with increasing Mn content is probably in close relation with the nature of Mn ion: different from divalent Mg, it is assumed that multivalent Mn ions dissolved in PMM'NZT can have other valences higher than 2 even though  $\text{Nb}^{5+}$  ions are co-doped for charge balance. On the whole, donor-like Mn ions occupying the perovskite B sites might cause the A-site vacancies  $V_{\text{Pb}}''$ [15], and retard grain growth by forming grain boundary adsorbed donor-vacancy associates[16]. This assumption will further be examined with the results of electrical property measurements.

Figures 5(a), (b), and (c) show the changes in  $k_p$ ,  $Q_m$  and  $\epsilon_{33}^T$  of PMM'NZT (Zr/Ti=47.5/52.5) with Mn/(Mg+Mn) ratio, sintered between 1100 and 1200 °C. All the specimens had fired densities fluctuating between 7.75 and 7.85  $\text{g}/\text{cm}^3$ , which were well over 97 % theoretical, and no tendency could be seen among relative density, composition and sintering condition. Electromechanical coupling factor  $k_p$  of 0.125PMN-0.875PZT was about 0.45, somewhat lower value than 0.6 of the same composition reported in the literature[3]. With increasing Mn content,  $k_p$  passed the peak value of  $\sim 0.56$  at Mn/(Mg+Mn)=0.317, and gradually decreased to  $\sim 0.48$  at end composition. Mechanical quality factor  $Q_m$  of 0.125PMN-0.875PZT revealed low value of 130, but was steeply increased to  $\sim 1400$  with the increase of Mn/(Mg+Mn) ratio up to 0.317, and dropped to  $\sim 1000$  at Mn/(Mg+Mn)=0.422, and then fluctuated at higher Mn contents. The relative permittivity  $\epsilon_{33}^T$ , in contrast, monotonically decreased with the increase of Mn content from  $\sim 1500$  at the starting composition to  $\sim 1000$  at the end point.

It is thought that the initial increases of  $k_p$  and  $Q_m$  at relatively low level of Mn are attributed to the complex doping effect of Mg and Mn, as was confirmed in PZT (52/48) doped with various complex impurity pairs[3]. The gradual decrease of  $k_p$  along with virtually constant  $Q_m$  in PMM'NZT with increasing Mn/(Mg+Mn) ratio over 0.317, however, cannot be explained with the well-known impurity doping effect[3] alone. According to this effect,  $\text{Mg}^{2+}$  and  $\text{Mn}^{2+}$  occupying B-sites of PZT act as acceptors and thus tend to enhance  $Q_m$  but reduce  $\epsilon_r$  and slightly degenerate  $k_p$ . Stoichiometric donor-doping of  $\text{Nb}^{5+}$  for charge compensation in the present study, however, would counterbalance these acceptor-doping effects[14]. Referring to the continuous decrease of  $\epsilon_{33}^T$  shown in Fig. 5(c), donor-like behavior of multivalent Mn ion previously suggested in the discussion of microstructure change in Fig. 4 seems not active to the electrical properties of PMM'NZT. As the data shown in

Figs. 5(a)-(c) are of the specimens with the same amounts of Mn+Mg and corresponding Nb, it is reasonable to think that the aforesaid changes in piezoelectric properties of 0.125PMM'N-0.875PZT with Mn/(Mg+Mn) ratio resulted from the substituting effect of donor-like Mn for Mg on internal bias as well as microstructure, both of which would influence the poling efficiency of PMM'NZT: The higher internal bias as well as the finer grain size of a piezoelectric ceramic has, the more difficult to pole it would become.

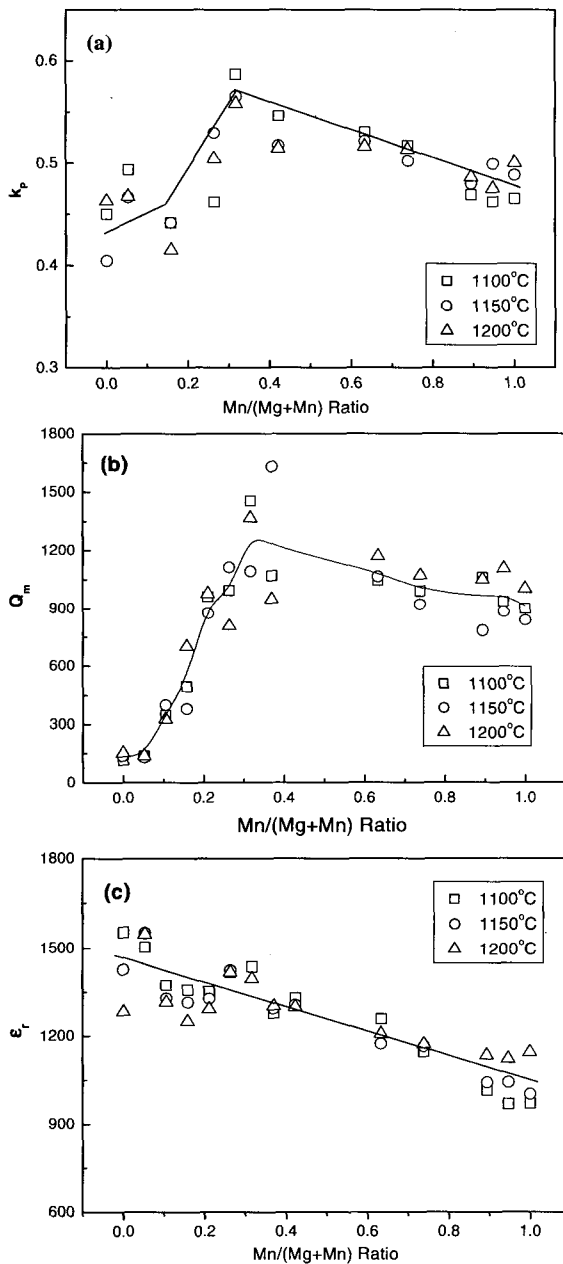


Fig. 5. Changes of (a)  $k_p$ , (b)  $Q_m$ , and (c)  $\epsilon_{33}^T$  of 0.125PMM'N-0.875PZT (Zr/Ti=47.5/52.5) with Mn/(Mg+Mn) ratio, sintered between 1100 and 1200 °C.

Figure 6(a) shows P-E hysteresis loops of PMM'NZT (Zr/Ti=47.5/52.5) of various Mn/(Mg+Mn) ratios, sintered at 1200 °C and aged for 24 h. All the compositions except Mn/(Mg+Mn)=1.0 revealed fully saturated but asymmetric loops, implying the formation of internal bias field[17]. Coercive field  $E_c$ , saturation polarization  $P_s$ , and internal bias field  $E_i$  of 0.125PMM'N-0.875PZT obtained with the loops are shown in Fig. 6(b). Hysteresis loop of 0.125PMM'N-0.875PZT (Mn/(Mg+Mn)=0.0) is quite symmetric, and thus its  $E_i$  value keeps relatively low at 140 V/cm. With increasing Mn content, the loop gradually changes to asymmetrical shape and  $E_i$  increases in correspondence while  $E_c$  remained virtually unchanged at ~2 kV/cm. On the other hand,  $P_s$  substantially increased up to Mn/(Mg+Mn) ratio of 0.317, and decreased at higher contents of Mn. The unsaturated polarization of 0.125PMM'N-0.875PZT stems from its extremely fine-grained microstructure (see Fig. 4(d)) as well as high  $E_i$ , both of which are thought responsible for the deterioration

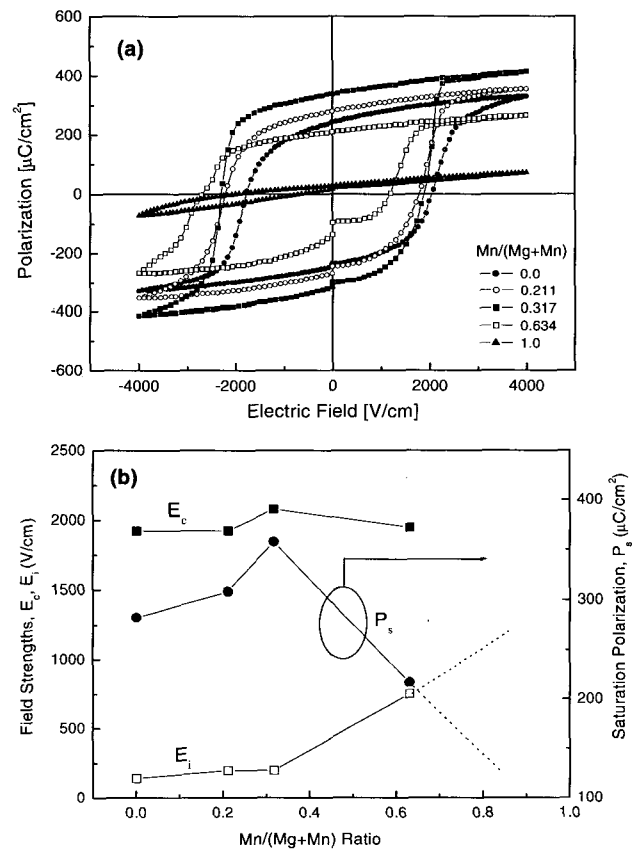


Fig. 6. (a) P-E hysteresis loops of 0.125PMM'N-0.875PZT (Zr/Ti=47.5/52.5) of various Mn/(Mg+Mn) ratios, and (b) their coercive fields ( $E_c$ ), saturation polarizations ( $P_s$ ), and internal bias fields ( $E_i$ ) as functions of Mn/(Mg+Mn) ratio, sintered at 1150 °C and aged for 24 h after poling.

of piezoelectric constants  $k_p$  and  $Q_m$  of PMM'NZT with high Mn contents. Microstructure and piezoelectricity of 0.125PMM'N-0.875PZT indicate that Mn/(Mg+Mn) ratio of 0.317 is the most promising for the transducer application. In this respect, the effect of Zr/Ti ratio on the piezoelectric properties of PMM'ZT with Mn/(Mg+Mn) ratio fixed at 0.317 was surveyed in detail.

Figures 7(a), (b), and (c) show  $k_p$ ,  $Q_m$ , and  $\epsilon_{33}^T$  of PMM'NZT (Mn/(Mg+Mn)=0.317) as functions of Zr/Ti ratio, respectively. Irrespective of Zr/Ti ratio, all the specimens showed relatively high densities between 7.80 and 7.85 g/cm<sup>3</sup>, but the grain size gradually increased with the increase of Zr/Ti ratio as shown in Fig. 4. Electromechanical coupling factor of the composition

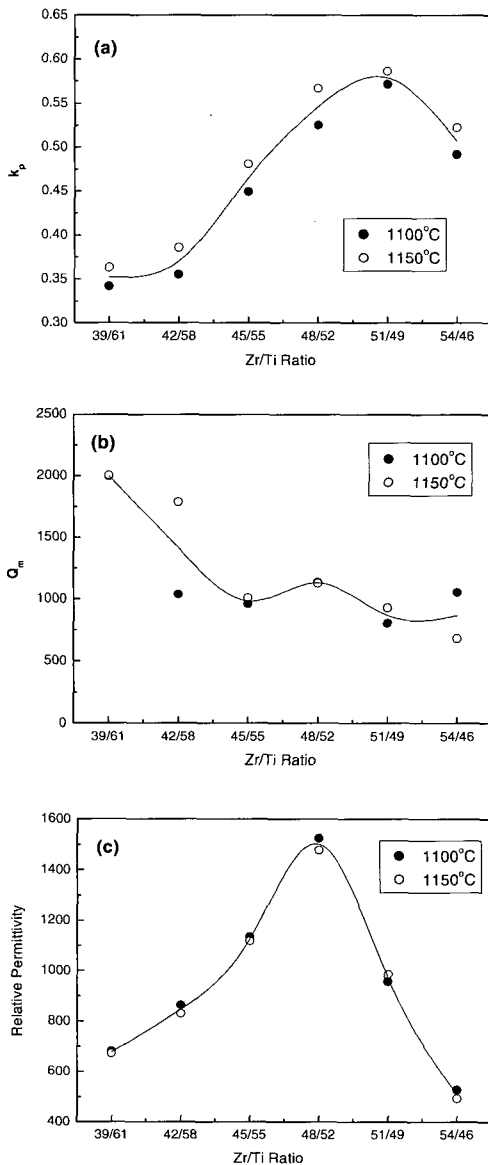


Fig. 7. Changes of (a)  $k_p$ , (b)  $Q_m$ , and (c)  $\epsilon_{33}^T$  of 0.125PMM'N-0.875PZT (Mn/(Mg+Mn)=0.317) with Zr/Ti ratio, sintered at (●): 1100 and (○): 1150 °C.

Zr/Ti=0.39 revealed low value of  $\sim 0.35$ , and was changed with Zr/Ti ratio:  $k_p$  reached the peak value of  $\sim 0.58$  near Zr/Ti=51/49 and fell to  $\sim 0.5$  at Zr/Ti=54/46.

Change in  $Q_m$  with Zr/Ti ratio showed an adverse tendency to  $k_p$ : starting composition had relatively high value of 2000, which decreased to  $\sim 1000$  at Zr/Ti=45/55 and leveled off. Relative permittivity was 700 in the starting composition. With increasing Zr/Ti ratio,  $\epsilon_{33}^T$  gradually increased and reached the peak value of 1500 at Zr/Ti=48/52, and then decreased to 500 at the end composition Zr/Ti=54/46.

In general, electrical properties of PZT depend strongly on its phase state: both  $k_p$  and  $\epsilon_r$  reveal peak values at the MPB due to increased polarizability of tetragonal-rhombohedral mixed phase;  $Q_m$ , in contrast, decreases at the MPB by the increase of domain wall mobility[3]. In the present PMM'NZT system, similar tendency has been confirmed but the composition of peak  $k_p$  did not coincide with that of peak  $\epsilon_{33}^T$ . With this discrepancy and the calculated lattice parameters shown in Fig. 3(b), it is concluded that the MPB of 0.125PMM'N-

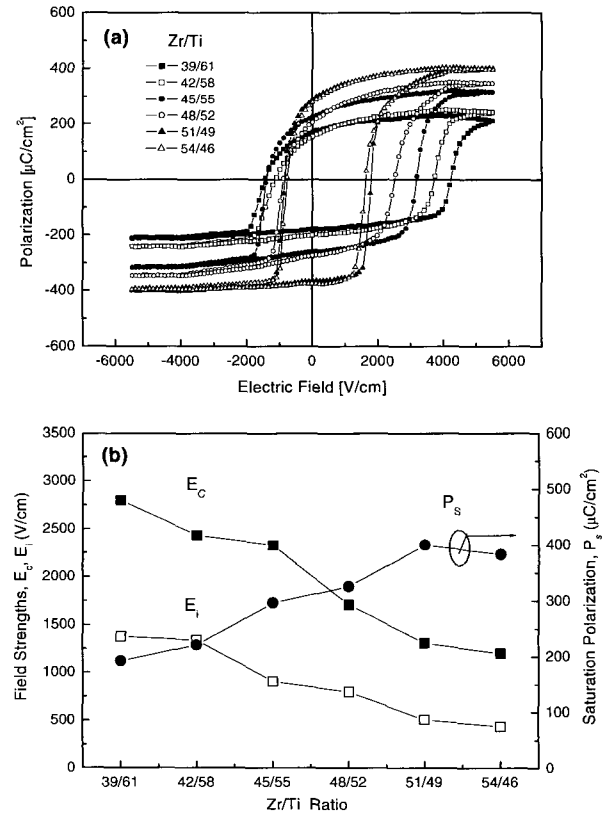


Fig. 8. (a) P-E hysteresis loops of 0.125PMM'N-0.875PZT (Mn/(Mg+Mn)=0.317) of various Zr/Ti ratios, and (b) their coercive fields  $E_C$ , saturation polarizations  $P_S$ , and internal bias fields  $E_i$  as functions of Zr/Ti ratio, sintered at 1150 °C and aged for 24 h after poling.

0.875PZT spans over relatively wide range of Zr/Ti ratio, in which optimal piezoelectricity appears at  $Mn/(Mg+Mn)=0.317$  and  $Zr/Ti=51/49$ .

Figure 8(a) shows P-E hysteresis loops of PMM'NZT ( $Mn/(Mg+Mn)=0.317$ ) of various Zr/Ti ratios, sintered at 1200 °C and aged for 24 h. All the compositions revealed fully saturated loops. The degree of symmetry of the loops, however, depended strongly on Zr/Ti ratio of the corresponding specimens. Coercive field ( $E_C$ ), saturation polarization ( $P_S$ ), and internal bias field ( $E_i$ ) of the specimens determined with the loops are shown in Fig. 8(b). Both  $E_C$  and  $E_i$  decreased while  $P_S$  increased with increasing Zr/Ti ratio. It implies that PMM'NZT becomes softer as its composition approaches the MPB.

The above results show that in 0.125PMM'N-0.875PZT system the composition  $Mn/(Mg+Mn)=0.317$  and  $Zr/Ti=51/49$  has some promising electrical properties for piezoelectric transformer application such as  $k_p=0.58$ ,  $Q_m \approx 1000$ , and  $\epsilon_{33}^T=970$ , as well as dense and fine-grained microstructure.

#### 4. CONCLUSION

In  $Pb(Mg_{1/3}Nb_{2/3})O_3[PMN]-Pb(Mn_{1/3}Nb_{2/3})O_3[PM'N]-PbZrO_3-PbTiO_3$  quaternary system (PMM'NZT) there were significant changes in the phase evolution, microstructure and the electrical properties such as  $k_p$ ,  $Q_m$  and  $\epsilon_{33}^T$  within the compositional ranges  $0 \leq y \leq 0.125$ ,  $y+z=0.125$ , and  $0.39 \leq x \leq 0.54$  of nominal formula  $Pb_{0.97}Sr_{0.03}[(Mg_{1/3}Nb_{2/3})_y(Mn_{1/3}Nb_{2/3})_z(Zr_xTi_{1-x})_{1-(y+z)}]O_3$ .

In case  $Mn/(Mg+Mn)$  ratio increased while Zr/Ti ratio being fixed at 47.5/52.5, phase relation was virtually unaffected but the grain size drastically decreased, and the electrical properties changed as following: both  $k_p$  and  $Q_m$  reached the peak values at  $Mn/(Mg+Mn)=0.317$ , and then gradually decreased;  $\epsilon_{33}^T$  decreased monotonically; P-E hysteresis loop gradually changed to asymmetrical shapes, and  $E_i$  increased in correspondence.

With increasing Zr/Ti ratio while fixing  $Mn/(Mg+Mn)$  ratio at 0.317, on the contrary, the cell parameter  $(a^2c)^{1/3}$  gradually increased, and tetragonal-rhombohedral MPB region appeared in the compositional range  $51/49 \leq Zr/Ti \leq 54/46$ . In the meantime, the electrical properties changed with increasing Zr/Ti ratio as following:  $k_p$  and  $\epsilon_{33}^T$  reached peak values at  $Zr/Ti=51/49$  and 48/52, respectively, and then gradually decreased; change of  $Q_m$  was adverse to  $k_p$ ; both  $E_C$  and  $E_i$  considerably decreased while  $P_S$  increased moderately. In consequence, PMM'NZT became softer as its composition approached the Ti-rich side of the MPB. In the system 0.125(PMN+PM'N)-0.875PZT studied, the composition  $Mn/(Mg+Mn)=0.317$  and  $Zr/Ti=51/49$  revealed superior electrical properties for piezoelectric

transformer application such as  $k_p=0.58$ ,  $Q_m \approx 1000$ , and  $\epsilon_{33}^T=970$ , as well as dense and fine-grained microstructure.

#### ACKNOWLEDGES

This research was supported by Kyungpook National University Research Fund, 1999.

#### REFERENCES

- [1] B. Jaffe, R. S. Roth, and S. Marzullo, "Piezoelectric properties of lead zirconate-lead titanate solid-solution ceramics", *J. Appl. Phys.*, Vol. 25, No. 6, p. 809, 1954.
- [2] G. A. Smolenskii and A. I. Agranovskaya, "Dielectric polarization and losses of some complex compounds", *Sov. Phys. -Tech. Phys.*, Vol. 3, No. 7, p. 1380, 1958.
- [3] Y. Xu, "Ferroelectric Materials and Their Applications", North-Holland Elsevier Science Publishers B.V., The Netherlands, p. 101, 1991.
- [4] S. Kawashima, "Piezoelectric ceramic inverter for LCD backlight", *Denshi-Gijutsu* (in Japanese), Vol. 3, p. 65, 1997.
- [5] H. Ouchi, K. Nagano, and S. Hayakawa, "Piezoelectric properties of  $Pb(Mg_{1/3}Nb_{2/3})-PbTiO_3-PbZrO_3$  solid solution ceramics", *J. Am. Ceram. Soc.*, Vol. 48, No. 12, p. 630, 1965.
- [6] H. Kawai, Y. Sasaki, T. Inoue, and S. Takahashi, "High power transformer employing piezoelectric ceramics", *Jpn. J. Appl. Phys. Part 1*, Vol. 35, No. 9B, p. 5015, 1996.
- [7] K. Ishii, N. Akimoto, S. Tashiro, and H. Igarashi, "Analysis of nonlinear phenomena in piezoelectric ceramics under high-power vibration", *J. Ceram. Soc. Japan* (in Japanese), Vol. 106, No. 6, p. 555, 1998.
- [8] F. Kulcsar, "Electromechanical properties of lead titanate zirconate ceramics modified with certain three- or five-valent additions", *J. Am. Ceram. Soc.*, Vol. 42, No. 1, p. 49, 1959.
- [9] S. L. Swartz and T. R. Shrout, "Fabrication of perovskite lead magnesium niobate", *Mat. Res. Bull.*, Vol. 17, No. 10, p. 1245, 1982.
- [10] IRE standards on piezoelectric crystals: measurements of piezoelectric ceramics, *Proc. IRE*, Vol. 49, No. 7, p. 1161, 1961.
- [11] E. Sawaguchi, "Ferroelectricity versus antiferroelectricity in the solid solutions of  $PbZrO_3$  and  $PbTiO_3$ ", *J. Phys. Soc. Japan*, Vol. 8, No. 5, p. 615, 1953.
- [12] D. R. Ride, "CRC Handbook of Chemistry and Physics", CRC Press, N.Y., p. F214, 1995.

- [13] P. Air-Gur and L. Benguigui, "X-ray study of the PZT solid solutions near the morphotropic phase transition", *Solid State Commun.*, Vol. 15, No. 6, p. 1077, 1974.
- [14] A. Boutarfaia, C. Boudaren, A. Mousser, and S. E. Bouaoud, "Study of phase transition line of PZT ceramics by X-ray diffraction", Vol. 21, No. 6, p. 391, 1995.
- [15] S. Takahashi, "Effects of impurity doping in lead zirconate titanate ceramics", *Ferroelectrics*, Vol. 41, p. 143, 1982.
- [16] K. H. Hardtl, "Electrical and mechanical losses in ferroelectric ceramics", *Ceram. Int.*, Vol. 8, No. 4, p. 121, 1982.
- [17] M. Takahashi, "Space charge effect in lead zirconate titanate ceramics caused by the addition of impurities", *J. Appl. Phys. Japan*, Vol. 9, No. 10, p. 1236, 1970.